Contribution of glutaredoxin-1 to Fas s-glutathionylation in ethanol-induced liver injury

Xiaomin Sun
Laboratory of Surgery, Children's Hospital of Chongqing Medical University, Chongqing, China. Ministry of Education Key Laboratory of Child Development and Disorders, Children's Hospital of Chongqing Medical University, Chongqing, China

Qin Deng
Laboratory of Surgery

Yunfei Zhang
Laboratory of Surgery, Children's Hospital of Chongqing Medical University, Chongqing, China

Jingyu Chen
Department of Ultrasound, Children's Hospital of Chongqing Medical University, Chongqing, China

chunbao guo (guochunbao@foxmail.com)
Children's Hospital of Chongqing Medical University

Research

Keywords: Ethanol, oxidant, glutaredoxin-1, protein s-glutathionylation, Fas

Posted Date: April 29th, 2020

DOI: https://doi.org/10.21203/rs.3.rs-24084/v1

Abstract

Background

The reversible glutathionylation modification (PSSG) of Fas augments apoptosis, which can be reversed by the cytosolic deglutathionylation enzyme glutaredoxin-1 (Grx1), but its roles in alcoholic liver injury remain unknown. Therefore, the objective of this study was to investigate the impact of genetic ablation of Grx1 on Fas-SSG in regulating ethanol-induced injury.

Methods

The role of Grx1 in alcoholic liver injury was investigated in Grx1 knockout mice. Alcoholic liver injury was achieved by feeding mice with a liquid diet containing 5% ethanol for 2 weeks.

Results

We demonstrated that ethanol-fed mice had increased Grx1 activity and oxidative damage in the liver. On the other hand, Grx1-deficient mice had more serious liver damage when exposed to ethanol compared to that of wild-type mice, accompanied by increased alanine aminotransferase and aspartate aminotransferase levels, Fas-SSG, cleaved caspase-3 and hepatocyte apoptosis. Grx1 ablation resulted in the suppression of ethanol-induced nuclear factor-κB (NF-κB) signaling, its downstream signal, and Akt signaling cascades, which are required for protection against Fas-mediated apoptosis. Accordingly, blocking NK-κB prevented Fas-induced apoptosis in WT mice but not Grx1-/- mice. Furthermore, the number of Kupffer cells and related proinflammatory cytokines, including Akt, were lower in Grx1-/- livers than those of the controls.

Conclusions

Grx1 is essential for adaptation to alcohol exposure-induced oxidative injury by modulating Fas-SSG and Fas-induced apoptosis.

Background

Ethanol consumption is a common health problem worldwide[1, 2]. Ethanol drinkers are usually susceptible to liver diseases, including liver steatosis, alcoholic hepatitis, cirrhosis, hypertension, and neuronal damage[3, 4, 5]. Ethanol-induced hepatocyte damage is characterized by high levels of reactive oxygen species (ROS), inflammatory cytokines, alanine aminotransferase (ALT) and aspartate aminotransferase (AST)[6, 7, 8]. During ethanol stress, free radicals are produced that exceed the antioxidant capacity of the liver[9], possibly modifying signal transduction, including apoptosis or

inflammatory signaling factors in a redox-dependent manner by specifically restoring the protein-SSG through glutaredoxin (Grx) [10, 11].

Various studies support the critical role of the Fas death pathway in liver injury[12, 13]. Fas is posttranslationally glutathionylated via the covalent attachment of glutathione (GSH), resulting in Fas-SSG. Fas-SSG enhances Fas recruitment and binding with FasL in lipid rafts, which was shown to be functionally important for promoting hepatocyte apoptosis[14, 15, 16]. While the mechanism of Fas-dependent cell death has clearly emerged, the detailed mechanism of redox-based s-glutathionylation of Fas during alcoholic liver injury is still unknown.

In the sinusoidal vascular space of the liver, Kupffer cells account for approximately 25 percent of nonparenchymal cells and can be activated to generate a variety of soluble factors and cytokines by many endogenous and exogenous stimuli [17, 18, 19]. Tumor necrosis factor α (TNF-α) is considered the most critical cytokine during alcoholic liver injury. Previous research indicated that depletion of TNF-α signaling could reverse alcohol-induced liver injury in mice[20, 21].

Here, we aimed to investigate the detailed mechanism by which redox-based s-glutathionylation of Fas promotes hepatic apoptosis in alcoholic liver injury. We also determined the contribution of Grx1 to Kupffer cell activation and inflammatory cytokine production in hepatic oxidative stress.

Materials And Methods

Animal experiment

The animal studies were conducted in accordance with the criteria approved by the Institutional Review Board and the Animal Care and Use Committee of Chongqing Medical University. Eight- to ten-week-old female Grx1-/- mice (kindly provided by Dr. Hongbo Luo of Harvard University), and the genetically corresponding wild-type (WT) mice were subjected to either a Lieber-DeCarli liquid diet containing 1–5% ethanol (volume/volume) or isocaloric amounts of pair-fed (PF) Lieber-DeCarli control diets over a period of two weeks. Then, on the last day, the mice were intragastrically administered 50% (v/v) ethanol every 20 minutes with an accumulated dosage of 5 g/kg body weight (Fig. 1).

In one set of experiments, the mice were treated with anti-FasL Ab (0.1 mg/mouse) (MFL4, BD PharMingen) through tail vein injections 24 hours before the first ethanol administration and again every three days. In another set of experiments, the mice were intraperitoneally (i.p.) injected either 1 mg/kg of BAY 11–7082 (EMD Chemicals, Gibbstown, NJ) or the control (DMSO in PBS 20% Tween-80) 24 hours before the first ethanol administration. The above time points were optimized based on several preliminary experiments. There were 3–6 mice in each experimental group. Consumption was recorded daily, and animal body weights were measured weekly. At 6 hours following the last dose of ethanol, the mice were euthanized. Blood and liver tissues were collected under sterile conditions. Some of the liver tissues were fixed and sliced for hematoxylin and eosin (H&E) staining and morphological examination.

Portions of the liver tissue were snap frozen in liquid nitrogen for quantitative real-time PCR (qPCR), Western blotting and biochemical assays. Tail snips were collected for genotyping.

Oil red O (ORO) staining

Oil red O (ORO) staining was performed as described previously [22]. Briefly, snap-frozen slides of liver sections were processed and stained with ORO solution. After washing in distilled water, the slides were subjected to H&E staining. Hepatic lipid droplets in H&E- and ORO-stained slides were observed under a light microscope.

Biochemical analysis

Abdominal aortic blood was collected, and serum ALT and AST levels were measured by commercial enzymatic assay kits (Diagnostic Chemicals, LTD, Oxford, CT) as previously described to detect liver damage [2]. Liver total cholesterol (TC) and triglyceride (TG) levels were assessed using commercially available reagents (California, United States).

GSH and GSSG measurement

The measurement protocol for reduced and oxidized glutathione was conducted as previously reported [22]. Glutathione (GSH) and oxidized glutathione (GSSG) were determined spectrophotometrically using GSH and GSSG assay kits (S0053, Beyotime). The ratio of GSH to GSSG (GSH/GSSG) is presented as nmol/mg protein and is an indicator of oxidative stress.

Dual confocal immunofluorescence detection of S-glutathionylated Fas

Dual confocal immunofluorescence staining and evaluation was performed as previously reported [22]. Briefly, the liver sections were incubated with the primary antibodies, (rabbit anti-GSH [Virogen] and goat anti-Fas antibody] [BD Biosciences]). The sections were then incubated with donkey anti-mouse Alexa Fluor 488 (Invitrogen) and donkey anti-rabbit Alexa Fluor 594 (Invitrogen) to develop immunofluorescence[22]. Finally, the nuclei were stained with DAPI (Sigma). During the experiment, the primary anti-GSH or anti-Fas antibodies were omitted as negative controls. The slides were observed via fluorescence confocal microscopy (Leica Microsystems, Heidelberg, Germany).

Superoxide Detection by Confocal Microscopy

The level of intracellular reactive oxygen species (ROS) was determined in liver slides through staining with the ROS-sensitive dye dihydroethidium (DHE) as previously described [22]. The liver sections were incubated with DHE for 30 min at 37 °C. The fluorescent signals (ROS, 488 nm; $O_2^{\bullet-}$, 535 nm) were visualized by a Leica TCS SP5 confocal microscope (Leica Microsystems, Heidelberg, Germany). The fluorescence intensity of random fields was analyzed by densitometry using ImageJ software (NIH) (at least 10 fields per sample). Three slides per animal and n = 3 per group were utilized.

Immunohistochemistry

Immunohistochemical assays were conducted according to previously described protocols [23]. Briefly, the slides were incubated with primary antibodies, including F4/80 (Abcam), at room temperature for 2 h. The expression of target proteins was visualized with a DAB peroxidase substrate kit (Vector Laboratories, Burlingame, CA).

Quantitative real-time PCR

RNA was extracted from snap-frozen liver tissues using TRIzol (Invitrogen, Carlsbad, CA) and then reverse transcribed (Omniscript; Qiagen, Hilden, Germany). Quantitative real-time PCR was performed on an ABI 7500 Real-Time PCR System (Applied Biosystems) using SYBR Green (Bio-Rad). The primer pairs and probes were used as previously reported[22]. The primers that were used to analyze the mRNA levels of IL-10, IL-12, MCP-1, IFN-γ and β-actin were designed using the Primer-BLAST system (www.ncbi.nlm.nih.gov/tools/primer-blast/) [5].

TUNEL assay

The paraffin-embedded sections were subjected to a terminal deoxynucleotidyltransferase-mediated dUTP-biotin nick-end labeling (TUNEL) assay using the APO-BrdU™TUNEL assay kit (Invitrogen) following the manufacturer's instructions. The TUNEL-positive cells were visualized under fluorescence microscopy.

ELISA analysis of active TNF-α in liver homogenate

Snap-frozen liver tissue samples (30–50 mg) were homogenized and centrifuged. The supernatants were used to detect the protein concentrations with a Pierce BCA kit (Thermo Scientific, Rockford, IL). The TNF-α concentration in liver homogenates was measured using a TNF-α Quantikine ELISA Kit (R&D Systems, Minneapolis, MN) according to the manufacturer's instructions.

Western Blotting

Snap-frozen tissues were first subjected to lysis buffer containing a protease inhibitor (Roche). Equal amounts of proteins (30 mg per lane) were separated on SDS-polyacrylamide gels (Invitrogen) and then transferred onto polyvinylidene difluoride (PVDF) membranes (Bio-Rad, Hercules, CA, USA) [23]. Afterwards, the membranes were incubated with specific diluted primary antibodies against the following proteins: RelA (Cell Signaling Technology, Boston, MA), RelB (Cell Signaling), IkBa (Santa Cruz), P-Akt (Santa Cruz), P-4E-BP1 (Santa Cruz), and β-Actin (Santa Cruz). After washing, the membranes were incubated with the appropriate horseradish peroxidase-conjugated secondary antibody for 1 h at room temperature. The densitometric analysis was conducted using ImageJ software (National Institutes of Health).

Grx1 Activity Assay

A glutaredoxin activity assay was conducted using a glutaredoxin fluorescent kit (11536, Cayman) according to the manufacturer's instructions.

Immunoprecipitation Assay

Tissue lysates were prepared from snap-frozen liver tissues according to the manufacturer's instructions (KeyGEN BioTECH). The protein concentration was determined by using the BCA method (P0010, Beyotime) and equalized for the immunoprecipitation assay[22]. The tissue lysate was then incubated with anti-glutathione antibody (Virogen) (2 μg/ml) overnight at 4 °C and immunoprecipitated by protein G agarose beads. The isolated immunoprecipitated proteins were then incubated with the anti-Fas antibody (Santa Cruz). For the control, dithiothreitol (DTT, 50 mM) was added to reduce S-glutathionylated proteins.

Statistical analysis

Statistical analysis was conducted with GraphPad Prism version 4 (GraphPad Software, Inc., La Jolla, CA). The results are expressed as the mean ± SEM. One-way ANOVA was performed for comparisons between groups in at least three independent experiments. Significance was defined as $P < 0.05$ and is indicated in the figure legends.

Results

1. Ethanol administration induced Grx1 activity in hepatic tissue

We first examined GSH and GSSG levels, which reflect ethanol-induced hepatic oxidative stress. The results showed significantly decreased GSH levels in ethanol-fed mice compared with those of pair-fed mice (Fig. 2A). Conversely, the GSSG level presented a marked increase (Fig. 2B). Correspondingly, the GSSG/GSH ratio increased from approximately 0.2 in the pair-fed mice to 1.8 in ethanol-fed mice, indicating hepatic oxidative stress (Fig. 2C). Grx1 depletion exacerbated this oxidative stress. We further evaluated oxidative production by detecting oxidized dihydroethidium (DHE) *in situ*. As indicated in Fig. 2D, there were similar DHE-derived fluorescence signals for Grx1 -/- and WT mice in the resting state. Ethanol exposure induced robust DHE-derived fluorescence, especially in Grx1 -/- mice (Fig. 2D), suggesting the involvement of Grx1 in oxidative stress.

Grx1 cleaves protein-GSH adducts, which constitute an important regulatory switch. We next investigated whether ethanol feeding influenced Grx1 activity. The results shown in Fig. 2E demonstrated that ethanol increased Grx1 activity following the last dose of ethanol(day 1), which persisted for 7 days compared with that of controls. As expected, in agreement with the results of Grx1 activity, increased Grx1 protein levels were detected by Western blot analysis in hepatic homogenates (Fig. 2F).

Grx1 depletion increased susceptibility to ethanol-induced hepatic injury

Next, we compared hepatic injury in Grx1-/- and WT mice with ethanol administration. As shown in Fig. 3A, the resting serum aspartate aminotransferase (AST), alanine aminotransferase (ALT), total cholesterol (TC) and triglyceride (TG) values were similar in Grx1 -/- and WT mice. Ethanol administration increased the serum ALT, AST, TC, and TG levels in the WT mice. Furthermore, ALT levels increased by 25%, TC levels increased by 15%, and TG levels increased by 35% in Grx1-/- mice compared with those of their WT counterparts (Fig. 3A, C, D). Although the AST level increased in response to alcohol, no difference between ethanol-fed Grx1-/- and WT mice was found (Fig. 3B). More steatosis (fat deposition) was present in the livers of ethanol-fed Grx1-/- mice compared with that of their WT counterparts, as indicated by H&E and Oil Red O staining (Fig. 3E, F), which was consistent with the biochemical analyses.

Grx1 depletion enhanced hepatic PSSG and Fas s-glutathionylation with ethanol exposure

We next investigated the importance of Grx1 in protein s-glutathionylation ethanol exposure. As shown in Fig. 4A, a slight increase in PSSG was observed in hepatic tissue in WT mice after ethanol exposure, whereas PSSG increased more robustly in Grx1-/- mice in the presence of ethanol under confocal laser scanning microscopy. Colocalization of Fas (green) and PSSG (red) indicated Fas-SSG formation (merge, yellow), which was predominantly located in hepatocytes (Fig. 34A) and Kupffer cells around the central veins. Ethanol exposure promoted an increase in the protein s-glutathionylation of Fas (yellow), with a further increase in Grx1-/- mice.

The immunoprecipitation assay showed significantly higher levels of Fas-SSG in whole-liver homogenates from ethanol-fed Grx1-/- mice compared with those of their WT counterparts. The specificity of the IP was confirmed with DTT (Fig. 4B, +DTT), with no immunoreactivity for Fas observed when DTT was used.

Grx1 ablation-induced apoptosis was Fas dependent

We then assessed ethanol-induced hepatic apoptosis using a terminal deoxynucleotidyl transferase dUTP nick end labeling (TUNEL) assay. As expected, ethanol-exposed mice exhibited higher rates of positive staining in hepatocytes, with marked increases in Grx1-/- mice compared to those of their WT counterparts (Fig. 5A), indicating severe hepatic injury in Grx1-depleted mice. Caspase-3 activation was higher in Grx1 ablation liver tissues than in their WT counterparts (Fig. 5B), which was similar to the results of the TUNEL assay. To demonstrate whether the TNF/FasL system is responsible for hepatic apoptosis, Fas L was blocked to confirm this cause-and-effect relationship. As shown in Fig. 5A and Fig. 5B, Fas L neutralization not only attenuated caspase-3 activation but also suppressed ethanol-induced apoptosis in Grx1-/- and WT mice. These results suggest that the TNF/FasL system plays a crucial role in ethanol-induced acute hepatic injury, which was modulated by Grx1.

Grx1 ablation enhanced Fas-induced apoptosis by NF-κB/Akt signaling

We next analyzed NF-κB/Akt signaling, which are key molecules implicated in Fas-induced liver injury. As shown in Fig. 6A, when exposed to ethanol, the expression of NF-kB family members and NF-κB-dependent cytokines increased in the Grx1-/- liver tissues compared with those of the WT counterparts. Consistent with the NF-κB signal, the p-Akt level (Ser473) in Grx1-/- livers was lower compared with that of the WT counterparts. Accordingly, the downstream target of p-Akt, eukaryotic translation initiation factor 4E-binding protein 1, was significantly increased in ethanol-exposed Grx1-/- mice compared with that of ethanol-exposed WT mice.

We further blocked NF-κB activity using BAY 11–7082 (BAY), a pharmacological inhibitor of NF-κB, to determine whether NF-κB activity is required for Fas-induced hepatocyte apoptosis. NF-κB neutralization not only prohibited caspase-3 activation (Fig. 6B) but also suppressed Fas-induced apoptosis (Fig. 6C) in WT mice but failed to further suppress caspase-3 activation and Fas-induced apoptosis in Grx1-/- mice.

Grx1 depletion alters Kupffer cells after ethanol exposure

Previous research suggested that Kupffer cells are the essential effectors in response to ethanol stress. We then addressed the involvement of Grx1 in Kupffer cells from pair- and ethanol-fed mice to explore the mechanism of monocyte or macrophage infiltration or apoptosis. As shown in Fig. 7A and 7B, the expression of F4/80, a marker of Kupffer cells, increased following ethanol exposure in WT mice, and in Grx1-/- mice, this increase was more pronounced, suggesting that the inflammatory cell infiltration induced by ethanol is exacerbated by Grx1 depletion. Ethanol also induced the expression of several proinflammatory cytokines (TNF-α, IL-10, and IL-12) in liver tissue from WT mice, and this increase was more pronounced in Grx1-/- mice (Fig. 7C). However, ethanol inhibited IFN-γ mRNA expression in hepatic tissues from both WT and Grx1-/- mice and had no effect on MCP1 mRNA expression in WT and Grx1-/- mice. Taken together, these results indicated that Grx1 was involved in ethanol-induced Kupffer cells activation and alterations in innate hepatic cytokines.

Discussion

Current research defines the mechanism of hepatocyte apoptosis as being controlled by the redox modulation system, which accounts for ethanol-induced liver injury. We demonstrated in this study that initial depletion of Grx1 brings about Fas s-glutathionylation during ethanol exposure, which promotes the aggregation and binding of Fas with FasL, and further activates caspases, resulting in apoptosis; these effects all occur via inactivation of the NF-κB/Akt pathway. To our knowledge, we observed the involvement of Grx1 in Fas-induced hepatocyte apoptosis for the first time. Moreover, our results showed that depletion of Grx1 in mice plays a critical role in ethanol-induced liver injury.

Oxidative stress is the main pathogenesis of ethanol-induced liver injury and exhibits a significant effect on the regulation of signaling proteins [21]. Oxidative stress modulates glutathione to the disulfide form[22, 23], and some reports have documented that ethanol exposure decreases GSH concentration [24] and restores GSH to normalize ALT *in vivo* [25, 26], suggesting that the imbalance in GSH due to oxidative stress contributes to hepatocyte injury. In the present study, we found a decrease in the GSH level and an increase in the GSSG-to-GSH ratio during ethanol-induced liver injury in conjunction with oxidative stress. Furthermore, the increase in GSSG favored s-glutathionylation through catalysis by the protein thiol oxidoreductase Grx1, which reduces mixed disulfide bonds, especially protein s-glutathionylation (PSSG) [27, 28]. Here, we reported that ethanol exposure induced Grx1 activity in liver tissue that specifically reduced GSH mixed disulfides, whereas Grx1 depletion promoted PSSGs, which might be associated with increases in apoptosis.

Grx1 has been implicated in various diseases, including chronic pulmonary disease, lung inflammation, *Pseudomonas aeruginosa* pneumonia, and hepatic warm I/R injury[29, 30, 31, 32]. The reducing power of Grx1 reverses protein oxidation, thereby potentially inhibiting the subsequent deleterious influence of the protein. We previously demonstrated enhanced Grx1 activity in intestinal tissue after the induction of NEC [22, 23] and that ablation of Grx1 resulted in enhanced intestinal injury [22]. Collectively, the current evidence [11, 33] demonstrated that Grx1 and s-glutathionylation function in diverse settings and play complex roles in disease pathogenesis. Because Grx1 has antioxidant and anti-inflammatory functions, it would be expected that Grx1 depletion would promote the susceptibility of the liver to injury. Herein, we demonstrated that Grx1 deletion promoted ethanol-induced liver injury in mice that manifested as increased plasma ASL and ALT levels and increased caspase activities.

Fas-induced apoptosis has been proposed to function in various liver diseases, such as ischemia/reperfusion injury, viral hepatitis, fulminant hepatic liver failure, and nonalcoholic and alcoholic steatohepatitis[34, 35, 36, 37]. Previous research suggested that s-glutathionylation of Fas results in robust Fas activation, which activates FasL-induced signaling and apoptosis [16, 38]. To date, the role of Grx1 in modulating Fas protein s-glutathionylation during ethanol stress has not been studied. In the present study, we demonstrated that after Grx1 ablation, increased s-glutathionylation of Fas overlapped with accelerated apoptosis that was consistent with ethanol-induced liver injury. We also demonstrated that these increases were normalized by FasL antibody, indicating an association with Fas s-glutathionylation and suggesting the involvement of the Grx1/Fas s-glutathionylation signaling axis in ethanol–induced liver injury.

In addition to the antioxidant effect, the Grx1/Fas axis might regulate the inflammatory signaling cascades that facilitate the function of Grx1 in ethanol-induced liver injury. Previous work demonstrated that nuclear factor-κB (NF-κB) was also dampened by *s*-glutathionylation, and Grx1 ablation further inhibited NF-κB activation [39, 40, 41]. In the current setting, NF-κB activation was reduced in ethanol-treated Grx1-ablated mice compared with that of WT mice, supporting the effect of Grx1 on NF-κB activity in the pathogenesis of ethanol-induced liver injury. NF-κB is well known as a proinflammatory transcription factor[42, 43, 44], and it could be inferred that NF-κB *s*-glutathionylation is responsible for

the phenotype and is involved in the molecular modulation observed in the present study. We observed that NF-κB blockade promoted Fas-induced hepatocyte apoptosis in WT mice but was unable to further enhance the effect of Grx1 ablation, which supported the role of the NF-κB redox state in mediating the antiapoptotic effects of Grx1. In addition, Akt has also been linked to the regulation of Grx1[45, 46], which was also observed in the present study. TNF-α is a downstream proinflammatory factor of NF-κB, which was confirmed to be necessary for liver injury induced by ethanol [47]. In the current study, Grx1 ablation further consolidated ethanol-induced increases in TNF-α mRNA and protein levels, which was normalized by blocking NF-κB, confirming the current hypothesis. Given the observations that the various inflammatory mediators mentioned above were regulated by Grx1 under ethanol exposure, we hypothesized that Grx1 normalizes rather than eliminates inflammatory cytokine activation, which may be a useful therapeutic target for ethanol exposure.

Under ethanol exposure, injured apoptotic cells are mostly hepatocytes, and there is the possibility that other immune cells within the liver may also undergo activation, including macrophages, infiltrating immune cells, and activated stellate cells. Here, we evaluated this hypothesis and demonstrated the hepatic macrophages accumulation and activation in ethanol-treated Grx1-/- mice. A previous report suggested that macrophage alternation in Fas-induced apoptosis accounted for increased inflammatory cytokines [48]. A low level of early proinflammatory cytokines (i.e., TNF-α) exhibited here was in accordance with the above scenario. Furthermore, inhibition of inflammatory cell apoptosis would result in an exacerbated inflammatory or fibrotic response[49, 50]. To our knowledge, this is the first report to explore Grx1 ablation-modulation of macrophage enrichment in the liver. However, our current study was limited in that we did not address the cellular specificity of immune cell apoptosis. Additional studies are required to assess these effects, which might be beyond the scope of the current research.

In conclusion, our study illuminated a new dimension of knowledge regarding Grx1, which plays an essential role in modulating ethanol-induced liver injury. The underlying mechanisms are related to redox-based regulation of Fas/FasL-induced apoptosis by multiple roles of Grx1 in the pathogenesis of ethanol exposure. Correspondingly, Grx1 might be a critical therapeutic target for treatment of ethanol-induced liver injury.

Abbreviations

ALT
alanine aminotransferase
AST
aspartate aminotransferase
DHE
dihydroethidium
Grx1
glutaredoxin-1
GSH

glutathione
NF-κB
nuclear factor-κB
ORO
Oil red O
PSSG
protein s-glutathionylation
ROS
reactive oxygen species
TNF-α
Tumor necrosis factorα
TC
total cholesterol
TG
triglyceride

Declarations

Declarations

* Ethics approval and consent to participate

Not required.

* Consent for publication

Our manuscript does not contain any identifiable individual's data in any form (including individual details, images or videos). That the article is original, has not already been published in a journal, and is not currently under consideration by another journal.

* Availability of data and material

The dataset analyzed during the current study are available from the corresponding author on reasonable request.

* Competing interests

No potential conflicts of interest relevant to this article are reported.

* Funding

This study was supported by grants from the National Natural Science Foundation of China (Nos: 30973440 and 30770950) in the design of the study, the Key Project of the Chongqing Natural Science Foundation (CSTC, 2008BA0021, cstc2012jjA0155) for collection, analysis, and interpretation of data and

the Chongqing Health Planning Commission of Research Fund (No: 2016MSXM044) in writing the manuscript.

* Authors' contributions

XS, QD, YZ and JC designed the study and analyzed the data. QD, YZ and JC evaluated the manuscript. CG and JC performed the statistical measurements and analyzed the data. CG analyzed the data and wrote the paper. All authors have read and approved the final manuscript as submitted and agree to be accountable for all aspects of the work.

* Acknowledgements

We thank Prof. Bailin Chen for providing technical assistance and for insightful discussions during the preparation of the manuscript and Dr Xiaoyong Zhang at the Wistar Institute for help with the linguistic revision of the manuscript.

* Authors' information (optional)

Xiaomin Sun and Qin Deng contributed equally to this study. Correspondence to Jingyu Chen or Chunbao Guo.

References

1. Ki SH, Park O, Zheng M, Morales-Ibanez O, Kolls JK, Bataller R, Gao B. Interleukin-22 treatment ameliorates alcoholic liver injury in a murine model of chronic-binge ethanol feeding: role of signal transducer and activator of transcription 3. Hepatology. 2010 Oct;52(4):1291–300.
2. Roychowdhury S, Chiang DJ, Mandal P, McMullen MR, Liu X, Cohen JI, Pollard J, Feldstein AE, Nagy LE. Inhibition of apoptosis protects mice from ethanol-mediated acceleration of early markers of CCl4 -induced fibrosis but not steatosis or inflammation. Alcohol Clin Exp Res. 2012 Jul;36(7):1139–47.
3. Seth D, Haber PS, Syn WK, Diehl AM, Day CP. Pathogenesis of alcohol-induced liver disease: classical concepts and recent advances. J Gastroenterol Hepatol. 2011 Jul;26(7):1089–105.
4. Cohen JI, Roychowdhury S, McMullen MR, Stavitsky AB, Nagy LE. Complement and alcoholic liver disease: role of C1q in the pathogenesis of ethanol-induced liver injury in mice. Gastroenterology. 2010 Aug;139(2):664–74. 674.e1.
5. Mandrekar P, Ambade A, Lim A, Szabo G, Catalano D. An essential role for monocyte chemoattractant protein-1 in alcoholic liver injury: regulation of proinflammatory cytokines and hepatic steatosis in mice. Hepatology. 2011 Dec;54(6):2185–97.
6. Louvet A, Mathurin P. Alcoholic liver disease: mechanisms of injury and targeted treatment. Nat Rev Gastroenterol Hepatol. 2015 Apr;12(4):231–42.

7. Gao B, Bataller R. Alcoholic liver disease: pathogenesis and new therapeutic targets. Gastroenterology. 2011 Nov;141(5):1572–85.
8. Mathews S, Xu M, Wang H, Bertola A, Gao B. Animals models of gastrointestinal and liver diseases. Animal models of alcohol-induced liver disease: pathophysiology, translational relevance, and challenges. Am J Physiol Gastrointest Liver Physiol. 2014 May;15(10):G819-23. 306(.
9. Kourkoumpetis T, Sood G. Pathogenesis of Alcoholic Liver Disease: An Update. Clin Liver Dis. 2019 Feb;23(1):71–80.
10. Nolin JD, Tully JE, Hoffman SM, Guala AS, van der Velden JL, Poynter ME, van der Vliet A, Anathy V, Janssen-Heininger YM. The glutaredoxin/S-glutathionylation axis regulates interleukin-17A-induced proinflammatory responses in lung epithelial cells in association with S-glutathionylation of nuclear factor κB family proteins. Free Radic Biol Med. 2014 Aug;73:143–53.
11. Ho YS, Xiong Y, Ho DS, Gao J, Chua BH, Pai H, Mieyal JJ. Targeted disruption of the glutaredoxin 1 gene does not sensitize adult mice to tissue injury induced by ischemia/reperfusion and hyperoxia. Free Radic Biol Med. 2007 Nov 1;43(9):1299 – 312.
12. Wang Y, Chen W, Han C, Zhang J, Song K, Kwon H, Dash S, Yao L, Wu T. Adult Hepatocytes Are Hedgehog-Responsive Cells in the Setting of Liver Injury: Evidence for Smoothened-Mediated Activation of NF-κB/Epidermal Growth Factor Receptor/Akt in Hepatocytes that Counteract Fas-Induced Apoptosis. Am J Pathol. 2018 Nov;188(11):2605–16.
13. Isayama F, Moore S, Hines IN, Wheeler MD. Fas Regulates Macrophage Polarization and Fibrogenic Phenotype in a Model of Chronic Ethanol-Induced Hepatocellular Injury. Am J Pathol. 2016 Jun;186(6):1524–36.
14. Anathy V, Aesif SW, Hoffman SM, Bement JL, Guala AS, Lahue KG, Leclair LW, Suratt BT, Cool CD, Wargo MJ, Janssen-Heininger YM. Glutaredoxin-1 attenuates S-glutathionylation of the death receptor fas and decreases resolution of Pseudomonas aeruginosa pneumonia. Am J Respir Crit Care Med. 2014 Feb;15(4):463–74. 189(.
15. Anathy V, Roberson E, Cunniff B, Nolin JD, Hoffman S, Spiess P, Guala AS, Lahue KG, Goldman D, Flemer S, van der Vliet A, Heintz NH, Budd RC, Tew KD, Janssen-Heininger YM. Oxidative processing of latent Fas in the endoplasmic reticulum controls the strength of apoptosis. Mol Cell Biol. 2012 Sep;32(17):3464–78.
16. Anathy V, Aesif SW, Guala AS, Havermans M, Reynaert NL, Ho YS, Budd RC, Janssen-Heininger YM. Redox amplification of apoptosis by caspase-dependent cleavage of glutaredoxin 1 and S-glutathionylation of Fas. J Cell Biol. 2009 Jan 26;184(2):241–52.
17. Sato K, Hall C, Glaser S, Francis H, Meng F, Alpini G. Pathogenesis of Kupffer Cells in Cholestatic Liver Injury. Am J Pathol. 2016 Sep;186(9):2238–47.
18. Gehring S, Dickson EM, San Martin ME, van Rooijen N, Papa EF, Harty MW, Tracy TF Jr, Gregory SH. Kupffer cells abrogate cholestatic liver injury in mice. Gastroenterology. 2006 Mar;130(3):810–22.
19. Li M, He Y, Zhou Z, Ramirez T, Gao Y, Gao Y, Ross RA, Cao H, Cai Y, Xu M, Feng D, Zhang P, Liangpunsakul S, Gao B. MicroRNA-223 ameliorates alcoholic liver injury by inhibiting the IL-6-

p47phox-oxidative stress pathway in neutrophils. Gut. 2017 Apr;66(4):705–15.

20. Yoo W, Lee J, Noh KH, Lee S, Jung D, Kabir MH, Park D, Lee C, Kwon KS, Kim JS, Kim S. Progranulin attenuates liver fibrosis by downregulating the inflammatory response. Cell Death Dis. 2019 Oct 7;10(10):758.
21. Ji C, Deng Q, Kaplowitz N. Role of TNF-alpha in ethanol-induced hyperhomocysteinemia and murine alcoholic liver injury. Hepatology. 2004 Aug;40(2):442–51.
22. Shang Q, Bao L, Guo H, Hao F, Luo Q, Chen J, Guo C. Contribution of glutaredoxin-1 to S-glutathionylation of endothelial nitric oxide synthase for mesenteric nitric oxide generation in experimental necrotizing enterocolitis. Transl Res. 2017 Oct;188:92–105.
23. Li X, Li X, Shang Q, Gao Z, Hao F, Guo H, Guo C. Fecal microbiota transplantation (FMT) could reverse the severity of experimental necrotizing enterocolitis (NEC) via oxidative stress modulation. Free Radic Biol Med. 2017 Jul;108:32–43.
24. Colell A, García-Ruiz C, Miranda M, Ardite E, Marí M, Morales A, Corrales F, Kaplowitz N, Fernández-Checa JC. Selective glutathione depletion of mitochondria by ethanol sensitizes hepatocytes to tumor necrosis factor. Gastroenterology. 1998 Dec;115(6):1541–51.
25. Ji C, Kaplowitz N. Betaine decreases hyperhomocysteinemia, endoplasmic reticulum stress, and liver injury in alcohol-fed mice. Gastroenterology. 2003 May;124(5):1488–99.
26. Ronis MJ, Butura A, Sampey BP, Shankar K, Prior RL, Korourian S, Albano E, Ingelman-Sundberg M, Petersen DR, Badger TM. Effects of N-acetylcysteine on ethanol-induced hepatotoxicity in rats fed via total enteral nutrition. Free Radic Biol Med. 2005 Sep 1;39(5):619 – 30.
27. Anathy V, Roberson EC, Guala AS, Godburn KE, Budd RC, Janssen-Heininger YM. Redox-based regulation of apoptosis: S-glutathionylation as a regulatory mechanism to control cell death. Antioxid Redox Signal. 2012 Mar;15(6):496–505. 16(.
28. Allen EM, Mieyal JJ. Protein-thiol oxidation and cell death: regulatory role of glutaredoxins. Antioxid Redox Signal. 2012 Dec 15;17(12):1748–63.
29. Peltoniemi MJ, Rytilä PH, Harju TH, Soini YM, Salmenkivi KM, Ruddock LW, Kinnula VL. Modulation of glutaredoxin in the lung and sputum of cigarette smokers and chronic obstructive pulmonary disease. Respir Res. 2006 Oct 25;7:133.
30. Kuipers I, Bracke KR, Brusselle GG, Aesif SW, Krijgsman R, Arts IC, Wouters EF, Reynaert NL. Altered cigarette smoke-induced lung inflammation due to ablation of Grx1. PLoS One. 2012;7(6):e38984.
31. Chia SB, Elko EA, Aboushousha R, Manuel AM, van de Wetering C, Druso JE, van der Velden J, Seward DJ, Anathy V, Irvin CG, Lam YW, van der Vliet A, Janssen-Heininger Y. Dysregulation of the glutaredoxin/S-glutathionylation redox axis in lung diseases. Am J Physiol Cell Physiol. 2019 Nov 6. doi:10.1152/ajpcell.00410.2019.
32. Jawad R, D'souza M, Selenius LA, Lundgren MW, Danielsson O, Nowak G, Björnstedt M, Isaksson B. Morphological alterations and redox changes associated with hepatic warm ischemia-reperfusion injury. World J Hepatol. 2017 Dec 8;9(34):1261–1269.

33. Aesif SW, Kuipers I, van der Velden J, Tully JE, Guala AS, Anathy V, Sheely JI, Reynaert NL, Wouters EF, van der Vliet A, Janssen-Heininger YM. Activation of the glutaredoxin-1 gene by nuclear factor κB enhances signaling. Free Radic Biol Med. 2011 Sep;15(6):1249–57. 51(.
34. Jing ZT, Liu W, Wu SX, He Y, Lin YT, Chen WN, Lin XJ, Lin X. Hepatitis B Virus Surface Antigen Enhances the Sensitivity of Hepatocytes to Fas-Mediated Apoptosis via Suppression of AKT Phosphorylation. J Immunol. 2018 Oct;15(8):2303–14. 201(.
35. Liu W, Jing ZT, Wu SX, He Y, Lin YT, Chen WN, Lin XJ, Lin X. A Novel AKT Activator, SC79, Prevents Acute Hepatic Failure Induced by Fas-Mediated Apoptosis of Hepatocytes. Am J Pathol. 2018 May;188(5):1171–82.
36. Item F, Wueest S, Lemos V, Stein S, Lucchini FC, Denzler R, Fisser MC, Challa TD, Pirinen E, Kim Y, Hemmi S, Gulbins E, Gross A, O'Reilly LA, Stoffel M, Auwerx J, Konrad D. Fas cell surface death receptor controls hepatic lipid metabolism by regulating mitochondrial function. Nat Commun. 2017 Sep 7;8(1):480.
37. Jia Z, Lian W, Shi H, Cao C, Han S, Wang K, Li M, Zhang X. Ischemic Postconditioning Protects Against Intestinal Ischemia/Reperfusion Injury via the HIF-1α/miR-21 Axis. Sci Rep. 2017 Nov;23(1):16190. 7(.
38. Doma E, Chakrabandhu K, Hueber AO. A novel role of microtubular cytoskeleton in the dynamics of caspase-dependent Fas/CD95 death receptor complexes during apoptosis. FEBS Lett. 2010 Mar 5;584(5):1033–40.
39. Reynaert NL, van der Vliet A, Guala AS, McGovern T, Hristova M, Pantano C, Heintz NH, Heim J, Ho YS, Matthews DE, Wouters EF, Janssen-Heininger YM. Dynamic redox control of NF-kappaB through glutaredoxin-regulated S-glutathionylation of inhibitory kappaB kinase beta. Proc Natl Acad Sci U S A. 2006 Aug;29(35):13086–91. 103(.
40. Pineda-Molina E, Klatt P, Vázquez J, Marina A, García de Lacoba M, Pérez-Sala D, Lamas S. Glutathionylation of the p50 subunit of NF-kappaB: a mechanism for redox-induced inhibition of DNA binding. Biochemistry. 2001 Nov;27(47):14134–42. 40(.
41. Jones JT, Qian X, van der Velden JL, Chia SB, McMillan DH, Flemer S, Hoffman SM, Lahue KG, Schneider RW, Nolin JD, Anathy V, van der Vliet A, Townsend DM, Tew KD, Janssen-Heininger YM. Glutathione S-transferase pi modulates NF-κB activation and pro-inflammatory responses in lung epithelial cells. Redox Biol. 2016 Aug;8:375–82.
42. Ghosh S, Hayden MS. New regulators of NF-kappaB in inflammation. Nat Rev Immunol. 2008 Nov;8(11):837–48.
43. Sun SC. The non-canonical NF-κB pathway in immunity and inflammation. Nat Rev Immunol. 2017 Sep;17(9):545–58.
44. Hatano E, Brenner DA. Akt protects mouse hepatocytes from TNF-alpha- and Fas-mediated apoptosis through NK-kappa B activation. Am J Physiol Gastrointest Liver Physiol. 2001 Dec;281(6):G1357-68.
45. Murata H, Ihara Y, Nakamura H, Yodoi J, Sumikawa K, Kondo T.Glutaredoxin exerts an antiapoptotic effect by regulating the redox state of Akt. J Biol Chem. 2003 Dec 12;278(50):50226–33.

46. Li Y, Liu W, Xing G, Tian C, Zhu Y, He F. Direct association of hepatopoietin with thioredoxin constitutes a redox signal transduction in activation of AP-1/NF-kappaB. Cell Signal. 2005 Aug;17(8):985–96.
47. Hakim MS, Ding S, Chen S, Yin Y, Su J, van der Woude CJ, Fuhler GM, Peppelenbosch MP, Pan Q, Wang W. TNF-α exerts potent anti-rotavirus effects via the activation of classical NF-κB pathway. Virus Res. 2018 Jul 15;253:28–37.
48. Schock SN, Young JA, He TH, Sun Y, Winoto A. Deletion of FADD in macrophages and granulocytes results in RIP3- and MyD88-dependent systemic inflammation. PLoS One. 2015 Apr 13;10(4):e0124391.
49. Ishii H, Adachi M, Fernández-Checa JC, Cederbaum AI, Deaciuc IV, Nanji AA. Role of apoptosis in alcoholic liver injury. Alcohol Clin Exp Res. 2003 Jul;27(7):1207–12.
50. Saile B, Knittel T, Matthes N, Schott P, Ramadori G. CD95/CD95L-mediated apoptosis of the hepatic stellate cell. A mechanism terminating uncontrolled hepatic stellate cell proliferation during hepatic tissue repair. Am J Pathol. 1997 Nov;151(5):1265–72.

Figures

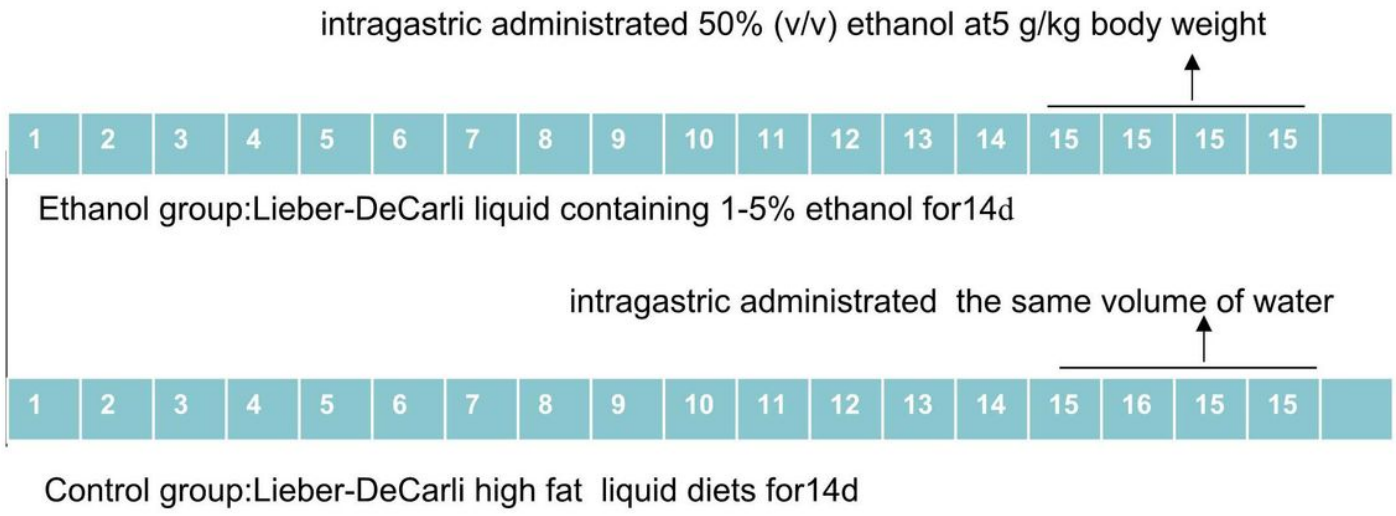

Figure 1

The experimental schemas of murine ethanol-induced liver injury

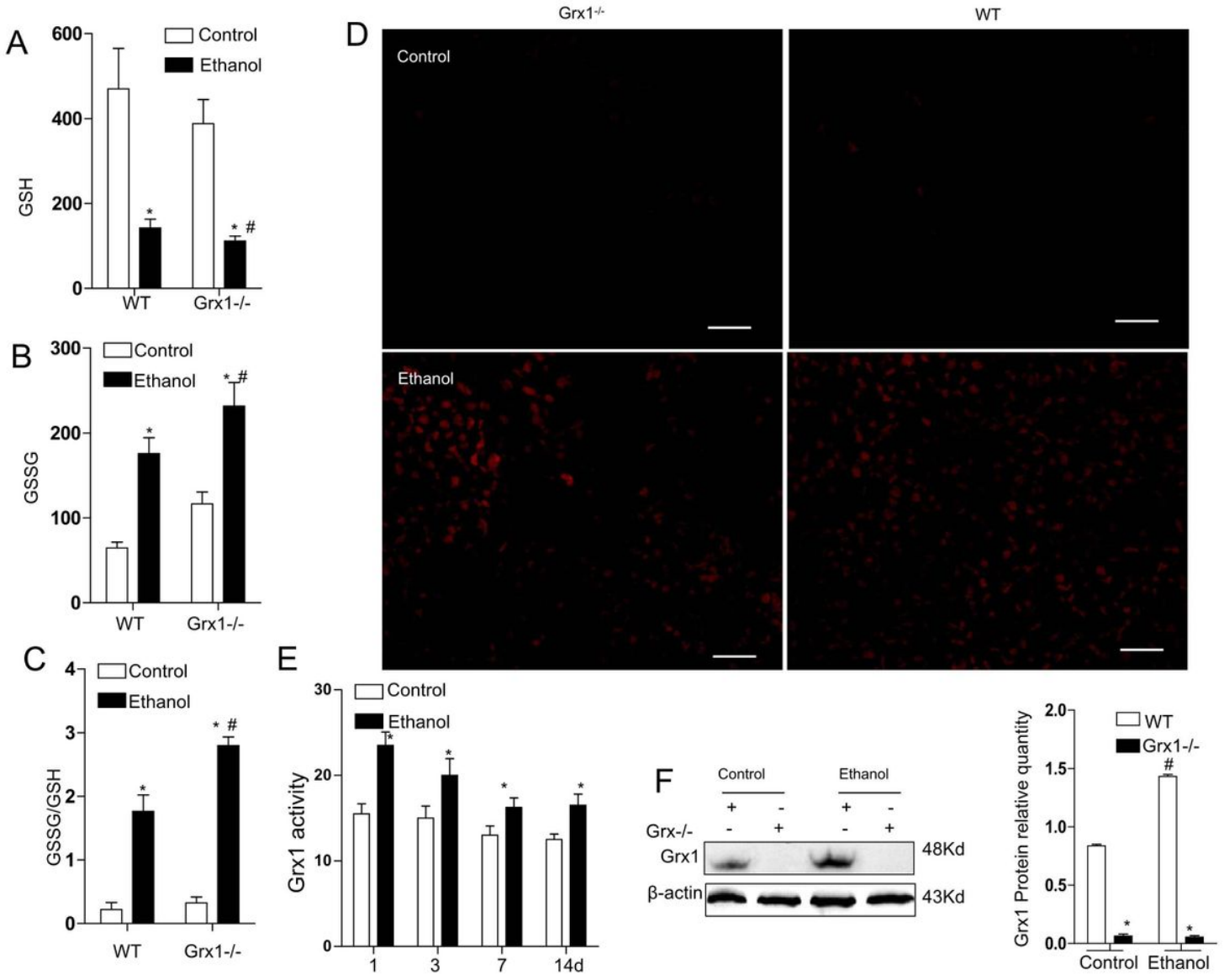

Figure 2

Assessment of hepatic oxidative stress and Grx1 activity after ethanol exposure. The levels of GSH (A) and GSSG (B) and the GSH-to-GSSG ratio (C) in the liver homogenates treated as indicated were determined as described in the Materials and Methods section. Columns represent the average values of 3 independent experiments; bars, standard error of the mean (SEM). *P<0.01 compared with the corresponding control groups (one-way ANOVA); # P <0.01 compared with ethanol-treated WT mice (one-way ANOVA). Grx1, glutaredoxin-1; GSH, glutathione; GSSG, oxidized GSH; NEC, necrotizing enterocolitis; WT, wild-type. (D) Fluorescent micrographs showing the detection of superoxide with dihydroethidine (DHE) in formalin-fixed liver sections, which is oxidized by O2 •− to a product with red fluorescence. Bar = 50 μm. The images are representative of at least 4 mice per treatment group and are shown. (E) At the time points indicated, Grx1 activity was evaluated in the liver homogenates that were treated as indicated. The data are expressed as the mean of four mice per group. *P<0.05 compared with the corresponding control groups (one-way ANOVA). (F) Western blotting for Grx1 in liver homogenates that were treated as indicated. β-actin was used as a loading control. Representative figures of multiple experiments with the

protein weights indicated (in kilodaltons) are shown. Right panel: Quantitative data of the relative intensity of Grx1 were calculated with respect to the loading control (assigned a value of 1). The data represent the means ± SEM. *P<0.05, compared with the corresponding control groups (one-way ANOVA). # P <0.01 compared with WT mice (one-way ANOVA).

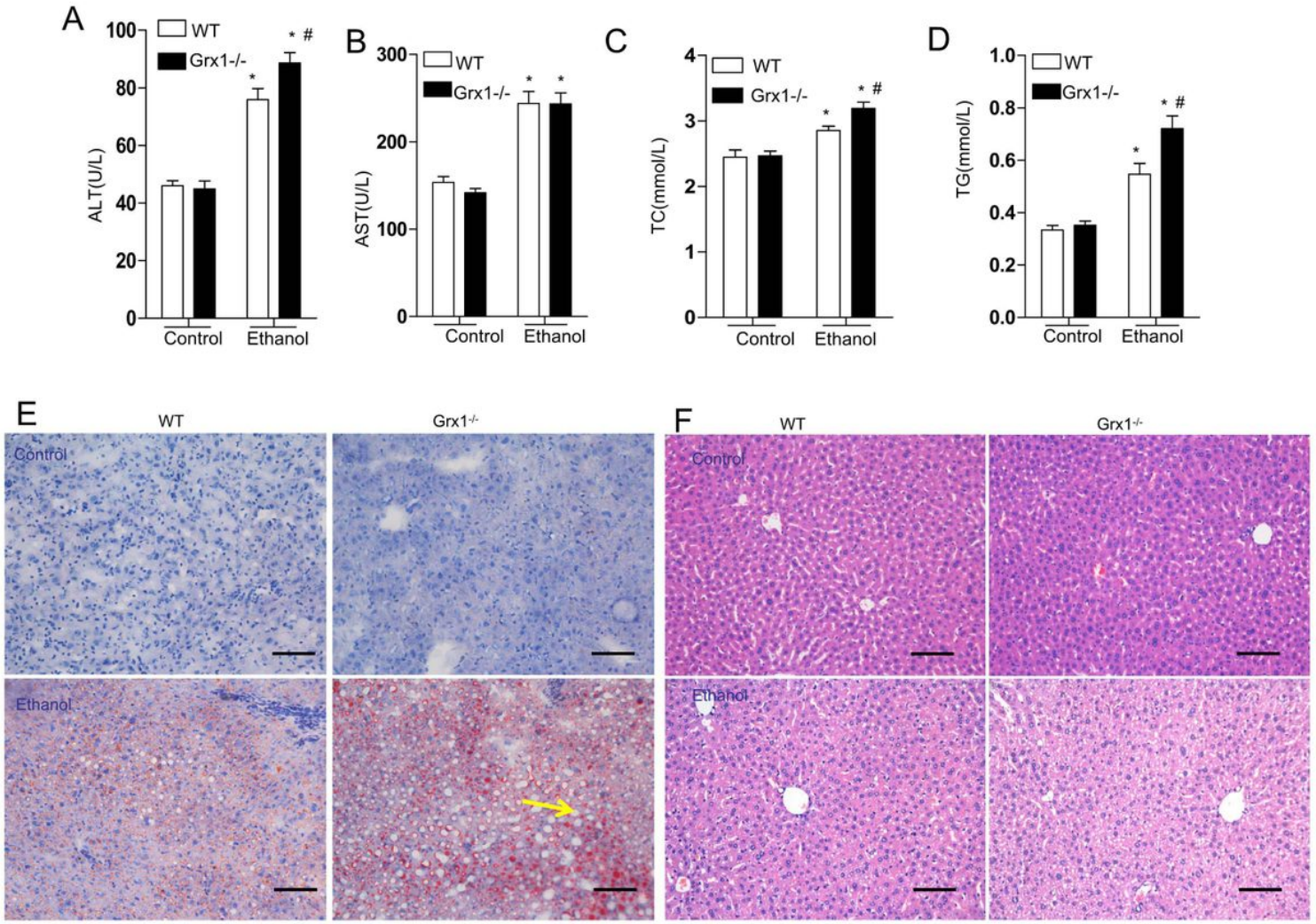

Figure 3

Grx1 ablation exacerbated ethanol-induced liver injury. The liver lesion was assessed by measuring serum ALT (A) and AST (B) in WT and Grx1-/- mice after binding. Hepatic steatosis was assessed by measuring serum total cholesterol (TC) (C) and triglyceride (TG) (D) levels. The data are represented as the mean±SEM (n=3/group). *P<0.01 compared with the corresponding control groups (one-way ANOVA); # P <0.01 compared with the ethanol-treated WT mice (one-way ANOVA). (E) Lipid accumulation in liver tissues that were treated as indicated; yellow arrowheads show refractile lipid droplets by oil red O staining (n = 3 animals for each group, 12 fields/animal). Scale bar = 50 μm. (F) Histologic sections of liver tissues that were treated as indicated were stained with H&E as described previously (n = 3 animals for each group, 12 fields/animal). Scale bar = 50 μm. One representative slide per group is shown.

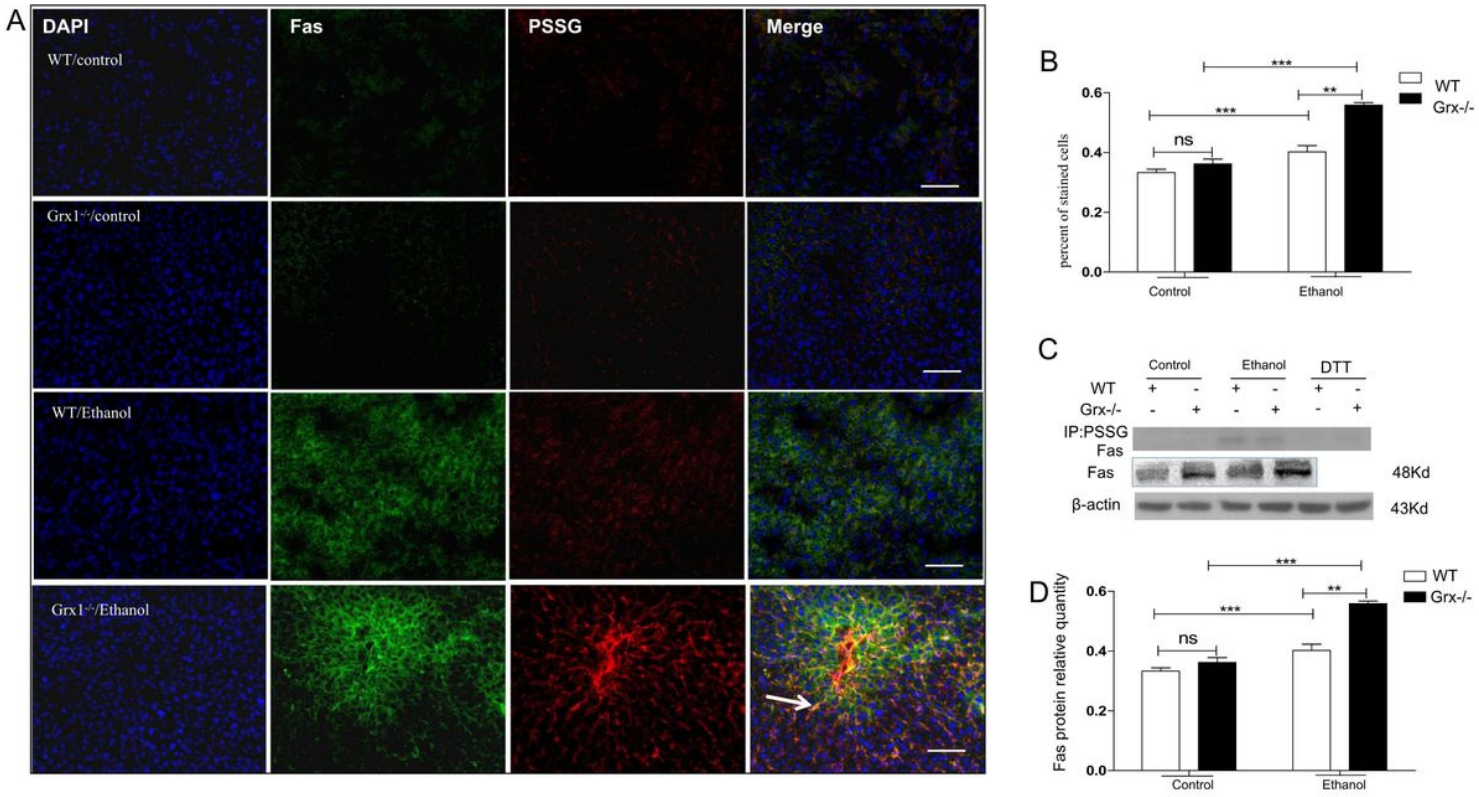

Figure 4

Assessment of Fas s-glutathionylation after ethanol exposure of WT and Grx1-/- mice. (A) Dual immunofluorescence staining was performed for Fas (left column, green fluorescence) and s-glutathionylation (second column, red fluorescence), and the merged images of the liver tissues that treated as indicated are shown. Colocalization of the cell markers is shown on the merged image, illustrating increased linking of Fas with PSSG (white arrows). Bar = 50 μm. (B) Quantification of Fas-SSG-positive cells was performed using a point-counting method and is expressed as the percentage of Fas-SSG-positive puncta divided by total parenchymal puncta. The data represent the means ± SEM. ***P<0.01, **P<0.01, compared with the corresponding control groups (one-way ANOVA). (C) The liver tissues were treated as indicated, dissected and mechanically homogenized and immunoprecipitated (IP) using an anti-glutathione (GSH) antibody. Precipitated proteins were resolved by reducing gel electrophoresis and probed using an anti-Fas antibody. As a control, the Grx1-/- sample was incubated with dithiothreitol (DTT) before electrophoresis. β-actin was selected as a loading control. (D) Quantitative data of the relative intensity of Fas were calculated with respect to the loading control (assigned a value of 1). The data represent the means ± SEM. ***P<0.01, **P<0.01, compared with the corresponding control groups (one-way ANOVA).

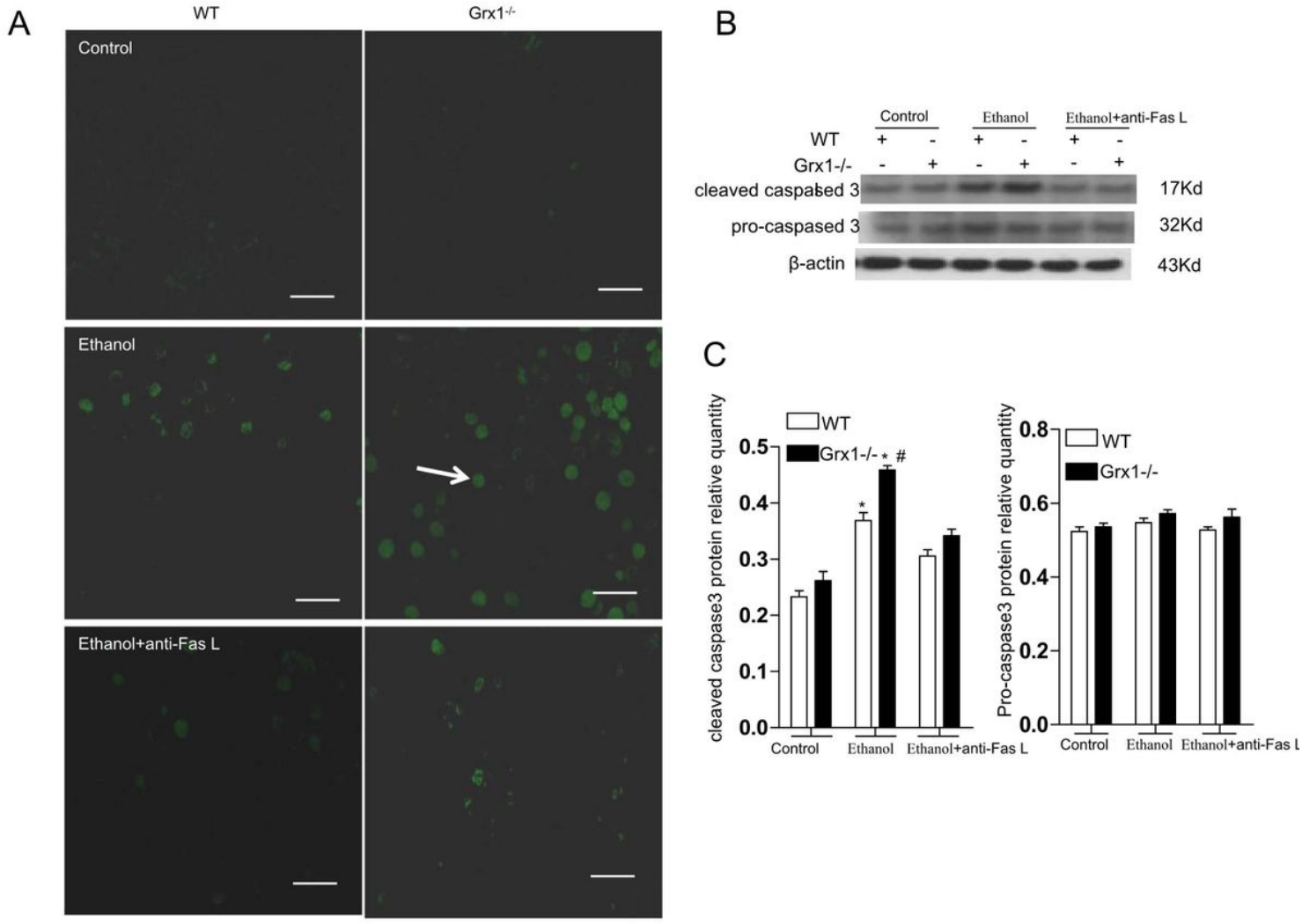

Figure 5

Grx1 ablation promoted apoptosis through the Fas pathway. (A) Representative confocal fluorescent images of formalin-fixed liver tissue obtained from the experimental mice that were treated as indicated to detect TUNEL-positive apoptotic hepatocytes (arrowheads). Scale bar = 50 μm. (B) Western blotting for multiple targets in the liver tissues obtained from experimental mice that were treated as indicated. β-actin was used as a loading control. Representative figures of multiple experiments are shown. (C) Quantitative data of the relative intensity of cleaved caspase 3 and pro-caspase 3 were calculated with respect to the loading control (assigned a value of 1). The data represent the means ± SEM. *P<0.01 compared with the corresponding control groups (one-way ANOVA); # P <0.01 compared with ethanol-treated WT mice (one-way ANOVA).

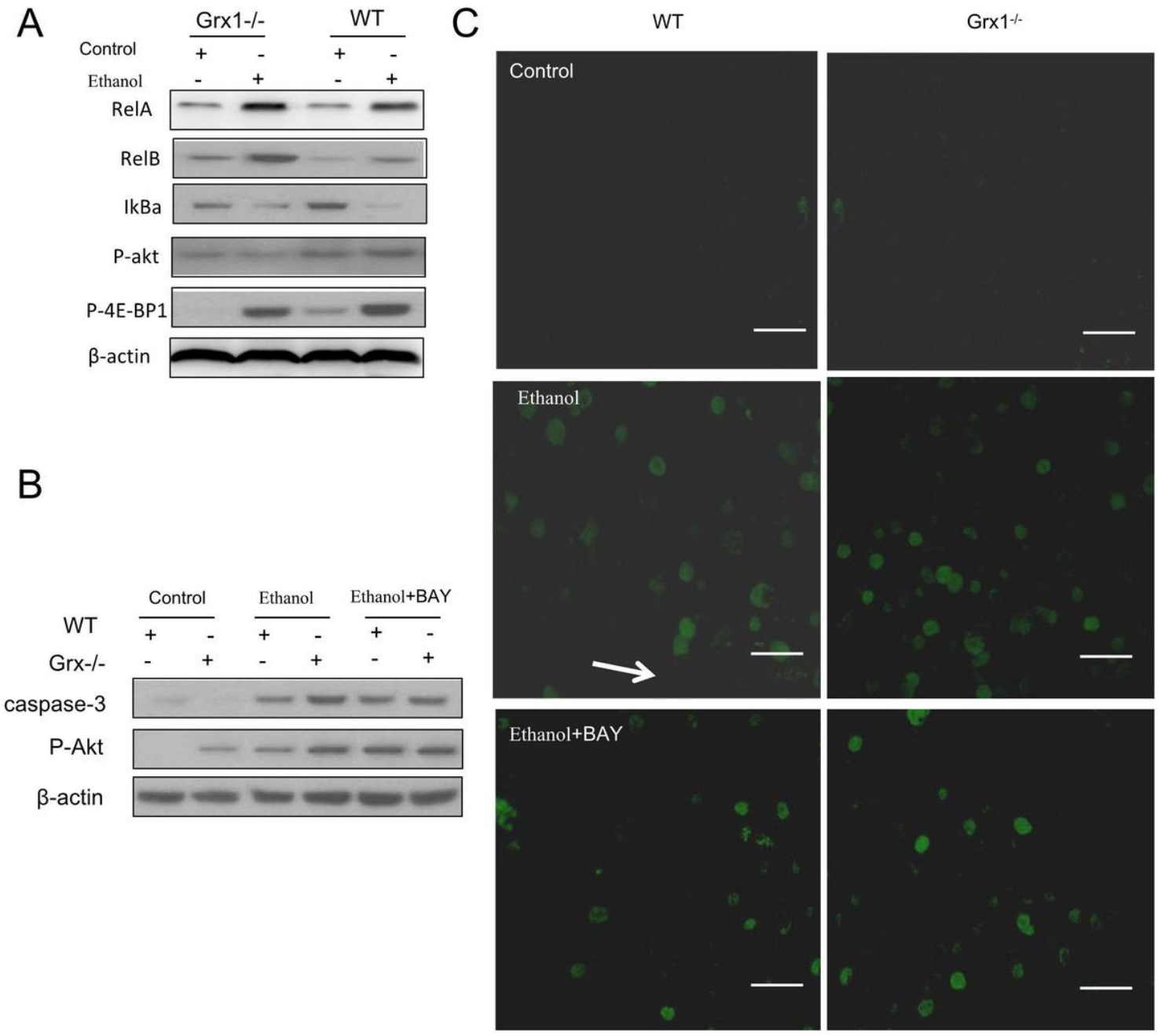

Figure 6

Blocking NF-kB promoted Fas-induced apoptosis. (A) Western blotting for multiple targets of the NF-kB/Akt signaling pathway, including RelA, RelB, IkBa, P-akt, and P-4E-BP1, in liver tissues obtained from experimental mice that were treated as indicated. β-actin was used as a loading control. Representative figures of multiple experiments are shown. (B) Western blotting for multiple apoptosis targets, caspase-3 and Akt, in liver tissues obtained from experimental mice that were treated as indicated. β-actin was used as a loading control. Representative figures of multiple experiments are shown. (C) Representative confocal fluorescent images of formalin-fixed liver tissue obtained from experimental mice that were treated as indicated to detect TUNEL-positive apoptotic hepatocytes (arrowheads). Scale bar = 50 μm.

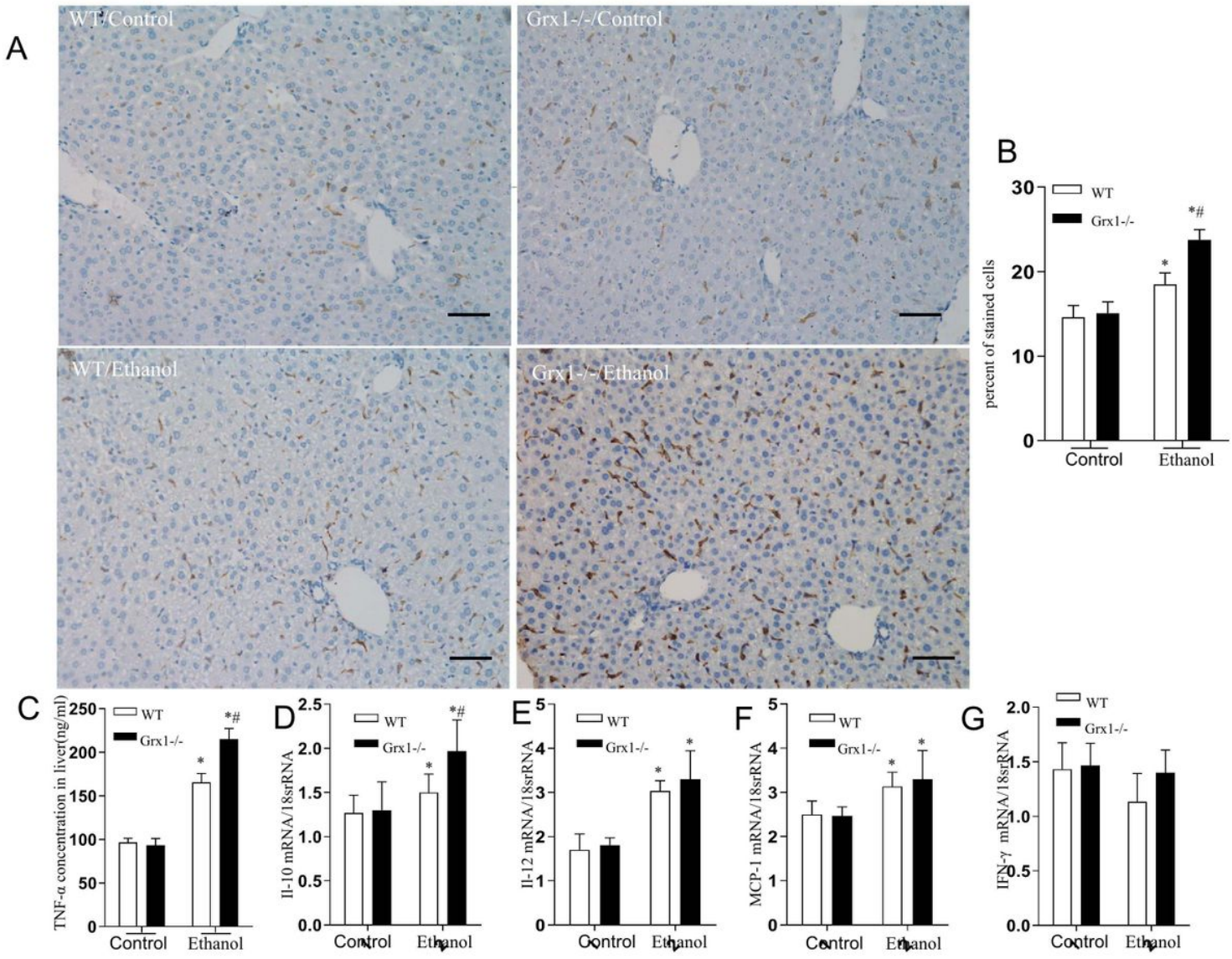

Figure 7

Grx1 ablation decreased Kupffer cells and proinflammatory factor expression. (A) F4/80-positive cell (Kupffer cell) distribution was detected by immunohistochemistry. Ten fields per section from each mouse were analyzed. Representative figures of multiple experiments are shown. Scale bar = 50 μm. (B) Semiquantitation of F4/80-positive cells is expressed as the percentage of F4/80-positive cells divided by total parenchymal cells. The data represent the means ± SEM. *P<0.01 compared with the corresponding control groups (one-way ANOVA); # P <0.01 compared with ethanol-treated WT mice (one-way ANOVA). (C) Quantitative RT-PCR of inflammatory cytokine transcripts in mice that were treated as indicated. The 18S RNA signal was used to normalize the signal of each gene transcript. The values are the mean ± SEM, *P<0.01 compared with the corresponding control groups (one-way ANOVA); # P <0.01 compared with ethanol-treated WT mice (one-way ANOVA).